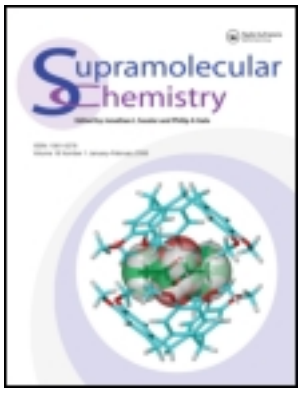

Supramolecular Chemistry
Publication details, including instructions for authors and subscription information:
http://www.tandfonline.com/loi/gsch20

Spontaneous self-assembly of designed cyclic dipeptide (Phg-Phg) into two-dimensional nano- and mesosheets

T. Govindaraju [a], M. Pandeeswar [a], K. Jayaramulu [b], Garima Jaipuria [c] & Hanudatta S. Atreya [c]

[a] Bioorganic Chemistry Laboratory, New Chemistry Unit, Jawaharlal Nehru Centre for Advanced Scientific Research, Jakkur, Bangalore, 560064, India

[b] Molecular Materials Laboratory, Jawaharlal Nehru Centre for Advanced Scientific Research, Jakkur, Bangalore, 560064, India

[c] NMR Research Centre, Indian Institute of Science, Bangalore, 560012, India

Available online: 03 May 2011

To cite this article: T. Govindaraju, M. Pandeeswar, K. Jayaramulu, Garima Jaipuria & Hanudatta S. Atreya (2011): Spontaneous self-assembly of designed cyclic dipeptide (Phg-Phg) into two-dimensional nano- and mesosheets, Supramolecular Chemistry, 23:7, 487-492

To link to this article: http://dx.doi.org/10.1080/10610278.2010.550685

Supramolecular Chemistry
Vol. 23, No. 7, July 2011, 487–492

Taylor & Francis
Taylor & Francis Group

Spontaneous self-assembly of designed cyclic dipeptide (Phg-Phg) into two-dimensional nano- and mesosheets

T. Govindaraju[a]*, M. Pandeeswar[a], K. Jayaramulu[b], Garima Jaipuria[c] and Hanudatta S. Atreya[c]

[a]*Bioorganic Chemistry Laboratory, New Chemistry Unit, Jawaharlal Nehru Centre for Advanced Scientific Research, Jakkur, Bangalore 560064, India;* [b]*Molecular Materials Laboratory, Jawaharlal Nehru Centre for Advanced Scientific Research, Jakkur, Bangalore 560064, India;* [c]*NMR Research Centre, Indian Institute of Science, Bangalore 560012, India*

(*Received 4 September 2010; final version received 16 December 2010*)

In this study, we present the spontaneous self-assembly of designed simplest aromatic cyclic dipeptides of (L-Phg-L-Phg) and (D-Phg-L-Phg) to form highly stable two-dimensional (2D) nano- and mesosheets with large lateral surface area. Various microscopy data revealed that the morphology of 2D mesosheets resembles the hierarchical natural materials with layered structure. Solution and solid-state NMR studies on cyclo(L-Phg-L-Phg) revealed the presence of strong (N—H—O) hydrogen-bonded molecular chains supported by aromatic $\pi-\pi$ interactions to form 2D mesosheets. Interestingly, cyclo(D-Phg-L-Phg) self-assembles to form single-crystalline as well as non-crystalline 2D rhomboid sheets with large lateral dimension. X-ray diffraction analysis revealed the stacking of (N—H—O) hydrogen-bonded molecular layers along *c*-axis supported by aromatic $\pi-\pi$ interactions. The thermogravimetric analysis shows two transitions with overall high thermal stability attributed to layered hierarchy found in 2D mesosheets.

Keywords: cyclic dipeptide; self-assembly; molecular chains; molecular layers; 2D sheets

1. Introduction

Molecular self-assembly-based bottom-up approach is a fascinating area of research for fabricating nano-, meso- and microscopic structures with unexplored properties (*1*). Biomolecules such as polypeptides, proteins, carbohydrates and lipids are the building blocks of a range of biological materials (*1*, *2*). These materials have essential biological functions such as structural stability, mechanical (cytoskeletal) strength, self-defence and many other physiological functions (*2*). An actively pursued area of research today involves the design of small organic molecules and peptides which self-assemble to form well-defined nano- and mesostructures with properties similar to natural materials (*3*, *4*). This is primarily due to the fact that peptides are modular in nature, and their structure and physicochemical properties can be tuned by chemical modifications to suit a desired application (*3*). Peptide-based materials find applications as biomaterials in cell culture, tissue engineering, stem cell growth, drug delivery and in the form of composite materials (*1*, *3*).

In recent years, a number of nanostructures formed by cyclic and acyclic peptides have been reported (*5*). The simplest cyclic forms comprise the cyclic dipeptides, which are more stable structurally and chemically compared to their acyclic congeners, and hence their nanostructures offer higher stability. Utility of cyclic dipeptides or their derivatives has been demonstrated with the formation of molecular chains (tapes) in crystalline form and macrocapsules in self-assembly-based aggregated forms (*6*). At the molecular level, cyclic dipeptide scaffolds can form hydrogen-bonded 1D chains or layers (*6*). Such structures are formed as a result of two pairs of (N—H—O) hydrogen bonds formed between two and four neighbouring molecules, respectively (Scheme 1). However, the formation of higher order self-assembled structures is not commonly observed. This is due to the fact that the absence of a suitable α-substituent (*R*, Scheme 1) to participate in intermolecular interactions prevents the formation of 2D extended structures by self-assembly (*7*, *8*). This can be accomplished by introducing additional orthogonal non-covalent interactions such as $\pi-\pi$ interactions involving aromatic groups at the α-position (*9, 10*). Design of such cyclic dipeptide molecules which self-organise via molecular chains and layers into nano- and mesosheets utilising aromatic $\pi-\pi$ interactions has not been studied, though formation of nanosheets formed by non-peptidic molecules such as metalloporphyrin, fullerene (C_{60}) and peptoids has been reported recently (*11–13*).

In this paper, we report for the first time the formation of 2D nano- and mesosheets by cyclic dipeptide (Phg-Phg) spanning several micrometers in lateral dimensions. The structural morphologies of the 2D sheets have been extensively characterised using different microscopy techniques such as field emission scanning electron

*Corresponding author. Email: tgraju@jncasr.ac.in

ISSN 1061-0278 print/ISSN 1029-0478 online

DOI: 10.1080/10610278.2010.550685
http://www.informaworld.com

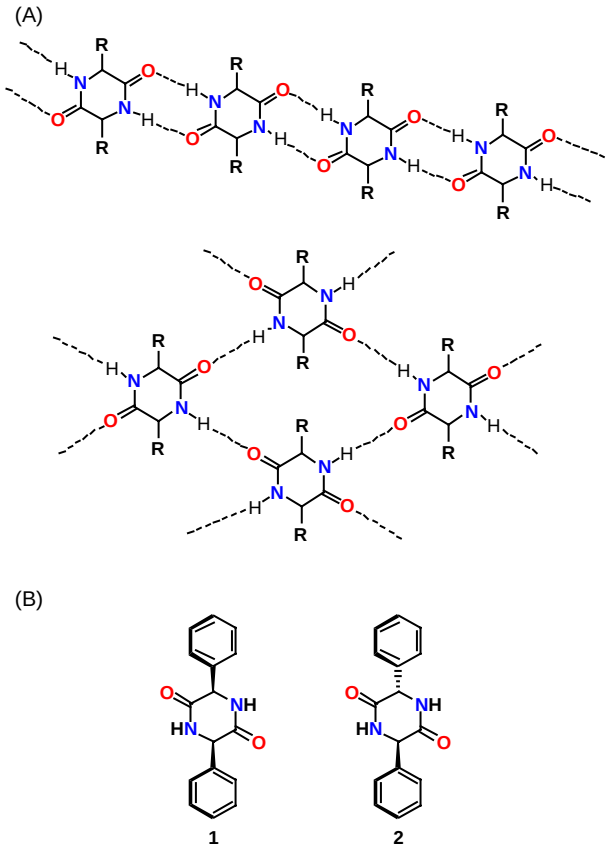

Scheme 1. Cyclic dipeptides form molecular chains (A) and molecular layers (B) through intermolecular (N—H—O) hydrogen bonding. Molecular structures of cyclic dipeptides of L-Phg-L-Phg (**1**) and D-Phg-L-Phg (**2**).

microscopy (FESEM), high-resolution transmission electron microscopy (HRTEM) and atomic force microscopy (AFM), by solution/solid-state NMR spectroscopy and single-crystal X-ray diffraction studies. Their hierarchy and morphology resemble that of natural materials with layered structure (*4b*, *c*) and are distinct from the earlier reports on cyclic and acyclic peptide-based nanomaterials.

2. Results and discussion

Cyclic dipeptides of L-Phg-L-Phg (**1**) and D-Phg-L-Phg (**2**) (Scheme 1) were prepared by coupling corresponding Fmoc-Phg-OH with H-Phg-OMe using peptide-coupling reagents.[1] The protected dipeptide (Fmoc-Phg-Phg-OMe) under Fmoc-deprotection conditions resulted in cyclo(Phg-Phg) **1** and **2** in quantitative yield, which spontaneously self-assembled to give insoluble 2D mesosheets with large lateral dimensions. In FESEM micrographs, 2D mesosheets with rhomboid shape and $>10\,\mu m$ lateral dimensions were observed (Figure 1(a)). This was further substantiated by HRTEM micrograph (Figure 1(b)), which revealed the existence of a layered

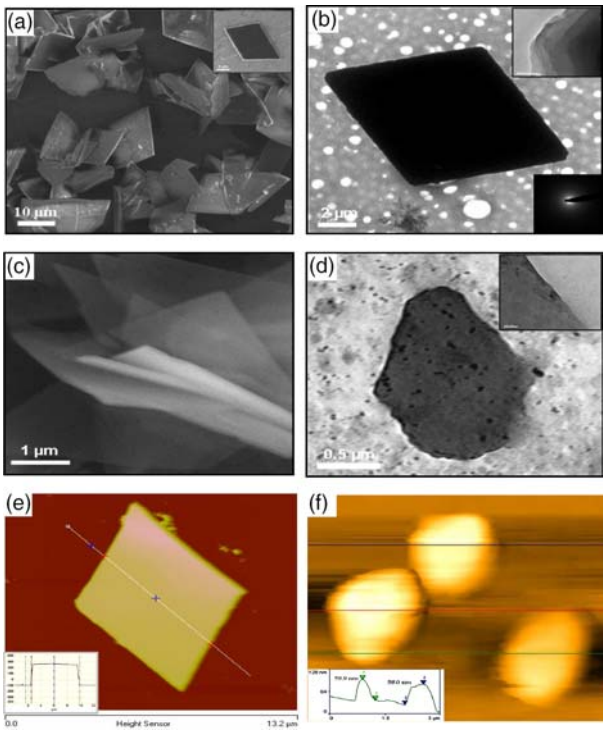

Figure 1. (a) FESEM micrograph of 2D mesosheets (inset shows the high-resolution image of an isolated mesosheet). (b) HRTEM micrograph of 2D mesosheet (inset shows the layered hierarchy (upper right) and non-crystalline nature of mesosheets as revealed by ED (lower right). FESEM (c) and HRTEM (d) micrograph of nanosheets formed from the solution of **1** in $CHCl_3$–TFA. Inset (d) high-resolution image of nanosheets showing smooth-layered surface. (e) AFM image of 2D mesosheet of **1** and inset show the corresponding height profile of 2D mesosheet (topographical thickness ~300 nm). (f) AFM image of 2D nanosheets formed from the solution of **1** in $CHCl_3$–TFA and corresponding height profiles (topographical layer thickness ~60 nm).

hierarchy (Figure 1(b), inset), and electron diffraction (ED, inset) revealed the non-crystalline nature of the 2D mesosheets. Attempts to solubilise the self-assembled mesosheets of **1** in organic solvents provided valuable insights. Cyclo(L-Phg-L-Phg) **1** was found to dissolve in $CHCl_3$ and CH_2Cl_2 upon acidification with trifluoroacetic acid (TFA). The solution of **1** in $CHCl_3$–TFA upon solvent evaporation formed well-separated 2D nanosheets (Figure 1(c) and (d)). Nanosheets were also obtained from the solution of **1** in CH_2Cl_2–TFA. The solvent evaporation leads to the formation of nanosheets exclusively and prevents the processes of further self-organisation to form mesosheets. This represents an indirect and alternative method for the exfoliation of nanosheets from 2D mesosheets. On the other hand, its acyclic congener (L-Phg-L-Phg) has been shown to form closed-cage nanospheres (*5f*). The 2D mesosheets possessed high thermal stability as determined from thermogravimetric analysis (TGA, Figure 2). The cyclo(L-Phg-L-Phg) **1** and

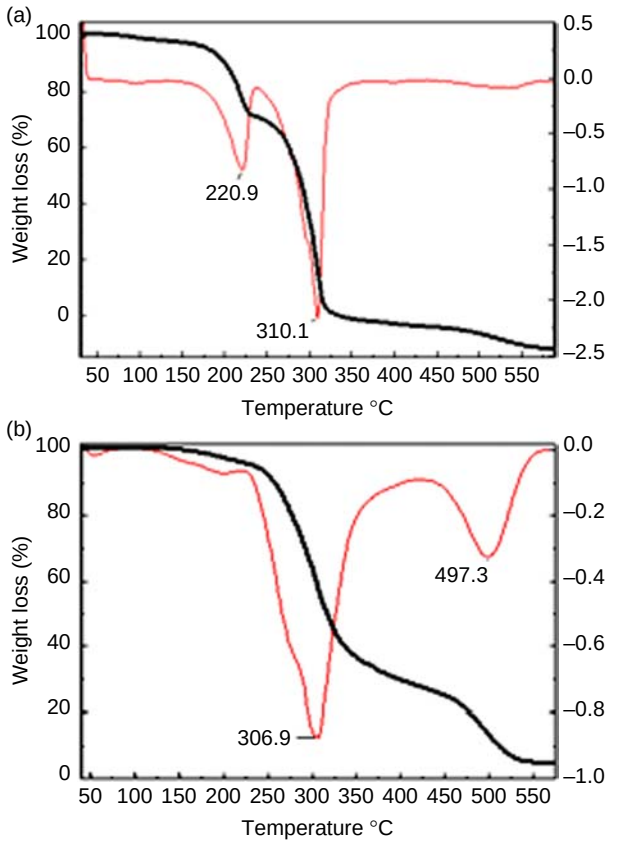

Figure 2. TGA of (a) cyclo(L-Phg-L-Phg) **1** 2D mesosheets and (b) cyclo(D-Phg-L-Phg) **2** 2D mesosheets. Main thermal transitions observed are at 220 and 310°C for **1** and 306 and 497°C for **2**. The weight losses are shown by the first derivative curve (red).

cyclo(D-Phg-L-Phg) **2** mesosheets (solid sample) showed two transitions which can be attributed to a hierarchical organisation of the 2D sheets.[1] The observed two characteristic thermal transitions correspond to transformation of mesosheets to nanosheets and then to complete decomposition. Major transitions were observed at 220 and 310°C for **1** (Figure 2(a)) and at 306 and 497°C for **2** (Figure 2(b)). High thermal decomposition temperatures clearly indicate the high stability associated with 2D mesosheets. This provides supporting evidence for the existence of morphological hierarchy involving the self-organised nanosheets to form stable mesosheets. The observed difference in the thermal stability of cyclic dipeptide **1** and **2** is predictably due to (N—H—O) and π–π interactions driven by 2D-extended molecular chains and molecular layers, respectively. Mesosheets of cyclic dipeptide **2** are composed of molecular layers with extended (N—H—O) hydrogen bonding network, that is reflected in their high thermal stability. However, mesosheets of cyclic dipeptide **1** are composed of linear molecular chains and show relatively lower transition temperatures.

AFM data also revealed the presence of 2D mesosheets with smooth and large lateral surface as shown in Figure 1(e). The height profile indicates a topographical thickness of ~300 nm with a well-defined rhomboid shape (Figure 1(e), inset). On the other hand, the AFM height profile of 2D nanosheets (formed by the solution of **1** in $CHCl_3$–TFA) indicates a layer thickness of ~60 nm (Figure 1(f)), suggesting that the nanosheets initially form by self-assembly of **1** which then self-organise to produce 2D mesosheets with large lateral surface area and sub-micrometre multi-layer thickness.

Solution and solid-state NMR spectroscopy was used to understand the different interactions involved at a molecular level (The details of the experimental set-up and the acquisition parameters used are provided in the Supplementary Material). First, the formation of monomeric cyclic dipeptide units was monitored by titrating a suspension of mesosheets of **1** in $CDCl_3$ with TFA until complete dissolution was obtained. Upon each addition (1 μl) of TFA (marked *i*–*v* in Figure 3(a) and (b)), 1D ^1H and 2D [^{15}N, ^1H] HSQC spectra were acquired. In the mesosheets, the amide protons ($^1H^N$) and ^{15}N have upfield shifts of 6.2 and 115 ppm, respectively. Such upfield shifts result from the ring-current effect in mesosheets as the amide protons are located in the shielding zone of closely stacked aromatic rings (Figure 3(f)). These resonances exhibit a shift to downfield regions of the spectrum upon addition of TFA (Figure 3(b)), which is attributed to disruption of intermolecular hydrogen bonds caused by the dissociation of sheets into monomeric units. This was further verified by acquiring 1D ^1H spectra for each addition of TFA at three different temperatures.[1] The amide proton temperature coefficients were observed to be -3 ± 0.1 ppb/K in mesosheets indicating strong hydrogen bonds (*14*) and -12 to -14 ppb/K upon dissolution in TFA. Thus, hydrogen-bond interactions present in the mesosheets are disrupted by the addition of TFA. Notably, on dissolution in $CDCl_3$–TFA, the amide proton showed cross-peaks arising from chemical exchange with the carboxylic proton of TFA in the 2D ROESY spectrum.[1] Furthermore, the *cis*-conformation of the two phenyl rings in cyclo(L-Phg-L-Phg) **1** (Figure 3(e)) was validated by the absence of a doublet for the $^1H^\alpha$ signal (Figure 3) due to three-bond scalar coupling to $^1H^N$ ($^3J(H^N–H^\alpha)$), implying that the ^3J is smaller than the line width of ~4 Hz. This is due to the fact that the *cis*-conformation results in the backbone torsion angle, Φ, to be almost 90° and hence $^3J(H^N–H^\alpha) \sim 0$ (*15*). The 1D ^1H–^{13}C CP and 2D ^1H–^{13}C heteronuclear correlation (HETCOR) experiments carried out in the solid state under magic angle spinning (MAS) (Figure 3(c) and (d)) provided ^{13}C chemical shifts in the 2D mesosheet form, which could not be obtained in solution due to low sensitivity. The $^{13}C^\alpha$ and ^{13}CO chemical shifts of ~60 and ~169 ppm, respectively, correspond to that observed in *cis*-amides of cyclic

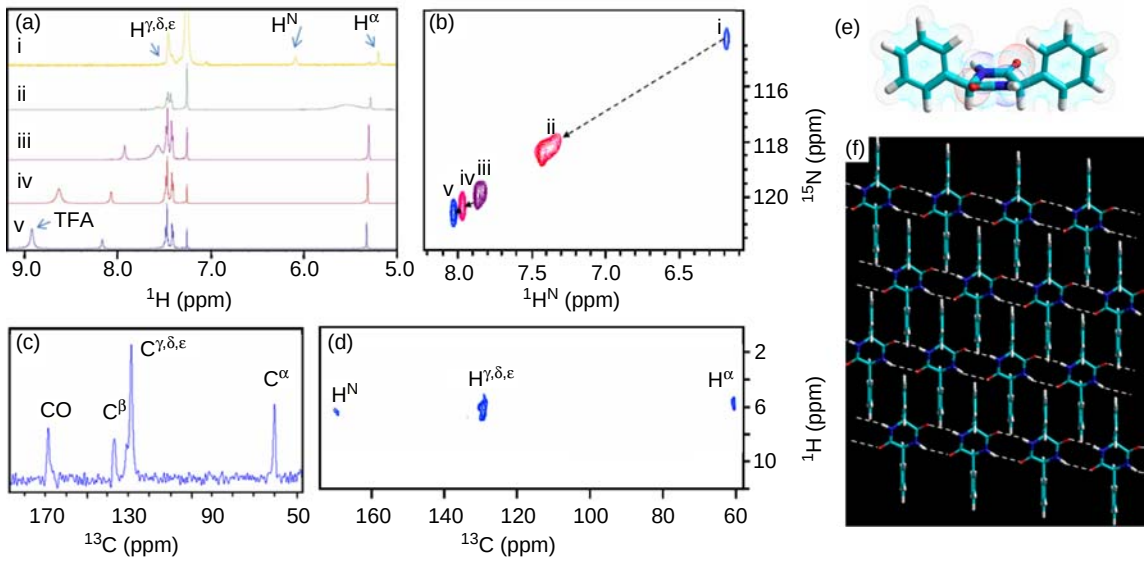

Figure 3. NMR characterisation of the 2D sheets. (a) 1D ^{1}H and (b) 2D [^{15}N,^{1}H] HSQC spectra acquired in the solution state at different additions of TFA. Chemical shift assignments of peaks are indicated. Spectra/peaks marked *i*–*v* in (a) and (b) indicate 0–3 and 5 μl additions of TFA, respectively. (c) ^{1}H–^{13}C CP. (d) 2D ^{1}H–^{13}C HETCOR spectra acquired in the solid state at a MAS rate of 11 kHz. (e) *cis*-conformation of cyclo(L-Phg-L-Phg) **1**. (f) A model of sheet formed by self-assembly of **1** through (N—H—O) hydrogen bonding and aromatic π–π interactions.

dipeptides (*16*). Evidently, the ^{1}H shifts of 5.3, 6.2 and 7.4–7.5 ppm for $^1H^\alpha$, $^1H^N$ and aromatic ^{1}H, respectively, obtained from 2D HETCOR match closely to the shifts observed in solution (Figure 3), thereby validating the solution-state NMR data.

Cyclo(D-Phg-L-Phg) **2** was also found to form 2D mesosheets similar to **1** with slightly reduced thickness (~200 nm).[1] Formation of nano-, meso- and microstructures through the processes of self-assembly-based aggregation as well as by the crystallisation of a cyclic or acyclic peptide with identical well-defined shape is a rare occurrence (*5a*, *17*). Though formation of self-assembled nanostructure of peptides has been explained using molecular packing determined from the crystallographic data, the actual shape of nano- or mesostructures differs considerably (*18*, *19*). However, the formation of 2D sheets has not been achieved through self-assembly-based aggregation and crystallisation with identical shapes. We succeeded in crystallising **2** into large 2D single-crystalline sheets as shown in Figure 4(a) using 2-methoxyethanol as a solvent. In contrast, non-crystalline 2D mesosheets of **2** suspended in methanol converted to single crystals with diamondoid shape over a period of 8 weeks. The crystal parameters obtained for diamondoid single crystals were similar to that of 2D single-crystalline sheets. The shape of 2D single-crystalline sheets resembled that of 2D mesosheets obtained by self-assembly-based aggregation as shown in Figure 1. These 2D single-crystalline sheets are much larger in dimension compared to non-crystalline 2D mesosheets. The lateral dimensions of rhomboid single-crystalline 2D sheets were found to be >600 μm as determined from the optical profiler analysis.[1] Cyclic dipeptide **2** crystallised in orthorhombic *P*bca space group, and structure determination[2] reveals that the dipeptide has two phenyl groups in reverse direction and that the dihedral angle between the phenyl rings is around 95°. The cyclic ring has two O═C—N—H parts on two sides, i.e. each unit has two H-bonding donor and two acceptor sites (Figure 4(b)). Therefore, each unit connects to the four different units by H7—N1 . . . O1 H—(N1..O1; 2.947(3) Å) bonding interactions, resulting in a 2D corrugated sheet (molecular layers, Figure 4(b)) lying in the crystallographic *ab* plane (Figure 4(b)). The cyclic dipeptide **2** stacks along the *c*-axis to form 2D single-crystalline sheet (Figure 4(c)). All the bond distances and angles are in the range of reported values in the literature. The arrangement of hydrogen-bonded molecular layers of **2** in two dimensions as a result of aromatic π–π interactions is shown in Figure 4(c). The single-crystalline 2D sheets do not possess layered structural hierarchy that was observed in non-crystalline 2D mesosheets obtained from self-assembly-based aggregation as shown in Figure 1(b).

3. Conclusion

This study demonstrates that the simplest aromatic cyclic dipeptides of (Phg-Phg) form well-defined 2D nano- and mesosheets with large lateral dimensions. The self-assembly of cyclo(L-Phg-L-Phg) **1** begins by formation of 2D nanosheets, followed by self-organisation of these nanosheets to form 2D mesosheets resembling the natural

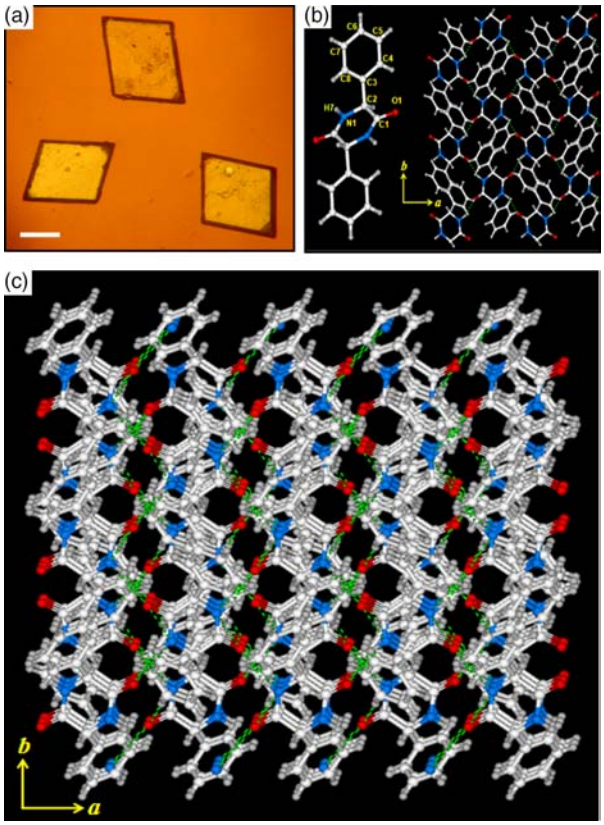

Figure 4. (a) Single-crystalline rhomboid 2D sheets of cyclo(D-Phg-L-Phg) **2** obtained from 2-methoxyethanol. The shape of these crystals is similar to that of 2D mesosheets formed by self-assembly-based aggregation. The single-crystalline 2D sheets are relatively larger in dimension (lateral dimension $>600\,\mu m$) compared to non-crystalline 2D mesosheets. Scale bar: 350 μm. (b) Ortep diagram and molecular interactions of cyclo(D-Phg-L-Phg) **2** to form molecular layers. (c) Packing of molecular layers along *c*-axis to form single-crystalline 2D sheet.

materials with layered structure. For the first time, we also demonstrated the formation of non-crystalline and single-crystalline 2D sheets with large lateral dimension using cyclo(D-Phg-L-Phg) **2**. The single-crystalline X-ray data revealed the presence of molecular layers that stacked along *c*-axis to form rhomboid 2D sheet. The highlight of this study is the large-scale production of 2D sheets from the smallest aromatic cyclic dipeptides which, in turn, can be obtained by a simple and straightforward synthetic route. The formation of nanosheets by solution of cyclo(Phg-Phg) in acidified organic solvent mixture such as $CHCl_3$–TFA is an indication that mesosheets consist of layered assembly of nanosheets and represents an easy route for the exfoliation of mesosheets. NMR and X-ray diffraction studies on **1** and **2** reveal that 2D sheets consist of a strong network of (N—H—O) hydrogen bonded molecular chains and molecular layers of cyclo(L-Phg-L-Phg) and cyclo(D-Phg-L-Phg), respectively, supported by aromatic π–π interactions. Taken together, the formation of such 2D sheets with large lateral surface area, their topographical hierarchy, high thermal stability and, in particular, strong hydrogen bonds along with aromatic π–π interactions open up new avenues for the design of novel biomaterials. For instance, 2D nano- and mesosheets of cyclo(Phg-Phg) can be viewed as potential candidates in applications such as biomineralisation, cell culture, tissue engineering, 2D sheet-derived composites and optoelectronic material scaffolds.

4. Experimental section

Complete experimental details can be found in the Supplementary Material, available online.

Acknowledgements

Authors thank Prof. C.N.R. Rao, FRS for constant support and encouragement, JNCASR and Department of Science Technology, Government of India, New Delhi, for financial support. We thank Prof. G.U. Kulkarni for FESEM, VIN lab for AFM facilities and Dr T.K. Maji for helping in X-ray crystallographic studies. We acknowledge Selvi, Basavaraja and Usha for their help in FESEM, AFM and TEM measurements.

Notes

1. See the Supplementary online material.
2. Crystal data of **2**: Formula $C_{16}H_{14}N_2O_2$, Mr = 266.29, orthorhombic, space group *P*bca (no. 61), $a = 10.1275(9)$ Å, $b = 8.2053(7)$ Å, $c = 15.5781(12)$ Å, $V = 1294.53(19)$ Å^3, $Z = 4$, ρcalc $= 1.366\,g\,cm^{-3}$, $\mu(Mo_{K\alpha}) = 0.092\,mm^{-1}$, $F(000) = 560$, $T = 293$ K, $\lambda(Mo_{K\alpha}) = 0.71073$ Å, $\theta_{max} = 22.2°$, total data = 6211, unique data = 815, $R_{int} = 0.084$, observed data $[I > 2\sigma(I)] = 588$, $R = 0.0383$, $R_w = 0.0983$, GOF = 1.04. CCDC 790250 contains the supplementary crystallographic data for this paper. This data can be obtained free of charge from The Cambridge Crystallographic Data Centre via www.ccdc.cam.ac.uk/data_request/cif.

References

(1) (a) Whitsides, G.M.; Grzvbowski, B. *Science* **2002,** *295*, 2418–2421. (b) Zhang, S. *Nat. Biotech.* **2003,** *21*, 1171–1178. (c) Chai, C.; Leong, K.W. *Mol. Ther.* **2007,** *15*, 467–480. (d) Langer, R.; Tirrell, D.A. *Nature* **2004,** *428*, 487–492. (e) Place, E.S.; Evans, N.D.; Stevens, M.M. *Nat. Mater.* **2009,** *8*, 457–470.

(2) (a) Branden, C.-I.; Tooze, J. *Introduction to Protein Structure*, 2nd ed., Garland, New York, 1999. (b) Meyers, M.A.; Chen, P.-Y.; Lin, A.Y.-M.; Seki, Y. *Prog. Mater. Sci.* **2008,** *53*, 1–206.

(3) (a) Gazit, E. *Chem. Soc. Rev.* **2007,** *36*, 1263–1269. (b) Ulijn, R.V.; Smith, A.M. *Chem. Soc. Rev.* **2008,** *37*, 664–675. (c) Brea, R.J.; Reiriz, C.; Granja, J.R. *Chem. Soc. Rev.* **2010,** *39*, 1448–1456.

(4) (a) Dankers, P.Y.W.; Meijer, E.W. *Bull. Chem. Soc. Jpn.* **2007,** *80*, 2047–2073. (b) Yang, X.; Dou, X.; Rouhanipour, A.; Zhi, L.; Räder, H.J.; Müllen, K. *J. Am. Chem. Soc.* **2008,** *130*, 4216–4217. (c) Rao, C.N.R.; Sood, A.K.; Subrahma-

nyam, K.S.; Govindaraj, A. *Angew. Chem., Int. Ed*. **2009,** *48*, 7752–7777.
(5) (a) Ghadiri, M.R.; Granja, J.R.; Milligan, R.A.; McRee, D.E.; Khazanovich, N. *Nature* **1993,** *366*, 324–327. (b) Bong, D.T.; Clark, T.D.; Granja, J.R.; Ghadiri, M.R. *Angew. Chem., Int. Ed*. **2001,** *40*, 988–1011. (c) Hartgerink, J.D.; Beniash, E.; Stupp, S.I. *Science* **2001,** *294*, 1684–1688; (d) Gelain, F.; Horii, A.; Zhang, S. *Macromol. Biosci.* **2007,** *7*, 544–551. (e) Reches, M.; Gazit, E. *Science* **2003,** *300*, 625–627. (f) Reches, M.; Gazit, E. *Nano Lett*. **2004,** *4*, 581–585.
(6) (a) Corey, R.B. *J. Am. Chem. Soc*. **1938,** *60*, 1598–1604. (b) MacDonald, J.C.; Whitesides, G.M. *Chem. Rev.* **1994,** *94*, 2383–2420. (c) Bergeron, R.J. *J. Am. Chem. Soc*. **1994,** *116*, 8479–8484. (d) Palmore, G.T.R.; Luo, T.-J.M.; McBride-Wieser, M.T.; Picciotto, E.A.; Reynoso-Paz, C.M. *Chem. Mater.* **1999,** *11*, 3315–3328. (e) Benedetti, E.; Corradini, P.; Pedone, C. *J. Phys. Chem*. **1969,** *73*, 2891–2895.
(7) Schwiebert, K.E.; Chin, D.N.; MacDonald, J.C.; Whitesides, G.M. *J. Am. Chem. Soc.* **1996**, *118*, 4018–4029.
(8) Palacin, S.; Chin, D.N.; Simanek, E.E.; MacDonald, J.C.; Whitesides, G.M.; McBride, M.T.; Palmore, G.T.R. *J. Am. Chem. Soc.* **1997**, *119*, 11807–11816.
(9) Joshi, K.B.; Verma, S. *Tetrahedron Lett.* **2008**, *49*, 4231–4234.
(10) Adler-Abramovich, L.; Aronov, D.; Beker, P.; Yevnin, M.; Stempler, S.; Buzhansky, L.; Rosenman, G.; Gazit, E. *Nat. Nanotech.* **2009**, *4*, 849–854.
(11) Wang, Z.; Li, Z.; Medforth, C.J.; Shelnutt, J.A. *J. Am. Chem. Soc.* **2007**, *129*, 2440–2441.
(12) Sathish, M.; Miyazawa, K.; Hill, J.P.; Ariga, K. *J. Am. Chem. Soc.* **2009**, *131*, 6372–6373.
(13) Nam, K.T.; Shelby, S.A.; Choi, P.H.; Marciel, A.B.; Chen, R.; Tan, L.; Chu, T.K.; Mesch, R.A.; Lee, B.-C.; Connolly, M.D.; Kisielowski, C.; Zuckermann, R.N. *Nat. Mater.* **2010**, *9*, 454–460.
(14) Cierpicki, T.; Otlewski, J. *J. Biomol. NMR* **2001**, *21*, 249–261.
(15) Kopple, K.D.; Ohnishi, M. *J. Am. Chem. Soc.* **1969**, *91*, 962–970.
(16) Deslauries, R.; Grzonka, Z.; Schaumburg, K.; Shiba, T.; Walter, R. *J. Am. Chem. Soc.* **1975**, *97*, 5093–5100.
(17) (a) Hartgerink, J.D.; Granja, J.R.; Milligan, R.A.; Ghadiri. M.R. *J. Am. Chem. Soc.* **1996,** *118*, 43–50. (b) Makabe, K.; Biancalana, M.; Yan, S.; Tereshko, V.; Gawlak, G.; Miller-Auer, H.; Meredith, S.C.; Koide, S. *J. Mol. Biol*. **2008,** *378*, 459–467.
(18) (a) Kar, S.; Drew, M.G.B.; Pramanika, A. *ARKIVOC* **2009,** *xii*, 43–59. (b) Leclair, S.; Baillargeon, P.; Skouta, R.; Gauthier, D.; Zhao, Y.; Dory, Y.L. *Angew. Chem., Int. Ed*. **2004,** *116*, 353–357. (c) Gupta, M.; Bagaria, A.; Mishra, A.; Mathur, P.I.; Basu, A.; Ramakumar, S.; Chauhan, V.S. *Adv. Mater.* **2007,** *19*, 858–861. (d) Zhu, P.; Yan, X.; Su, Y.; Yang, Y.; Li, J. *Chem. Eur. J.* **2010**, *16*, 3176–3183. (e) Görbitz, C.H. *Chem. Eur. J*. **2001,** *7*, 5153–5159.
(19) (a) Görbitz, C.H.; Nilsen, M.; Szeto, K.; Tangen, L.W. *Chem. Commun*. **2005,** 4288–4290. (b) Görbitz, C.H. *Chem. Eur. J*. **2007,** *13*, 1022–1031. (c) Luo, T.-J.M.; Palmore, G.T.R. *J. Phys. Org. Chem*. **2000,** *13*, 870–879.